ISBN: 978-3-95450-231-8 ISSN: 2673-5490 doi: 10.18429/JACoW-IPAC2023-MOPA040

CLOSING CRAB DISPERSION BY DISPERSIVE RF CAVITY IN ELECTRON-ION COLLIDER HADRON STORAGE RING *

D. Xu†, , Y. Luo, J. S. Berg, H. Lovelace III, S. Tepikian, Q. Wu,
B. Xiao, J. Avronsart, H. Witte, M. Blaskiewicz, C. Montag, F. Willeke
Brookhaven National Laboratory, Upton, NY, USA
B. R. Gamage, Jefferson Lab, Newport News, VA, USA
V. Morozov, Oak Ridge National Lab, Oak Ridge, TN, USA
Y. Hao, Michigan State University, East Lansing, MI, USA

Abstract

The Electron-Ion Collider (EIC) uses the local crab crossing scheme to compensate the geometric luminosity loss of the 25 mrad crossing angle in the interaction point. Due to space limitations and other optics constraints, the beam optics at the crab cavities in the Hadron Storage Ring (HSR) is not perfectly matched to fully compensate the crab dispersion. This paper discusses the possibility of closing the crab dispersion by a dispersive RF cavity. The formula is derived and the required momentum dispersion at the RF cavity is calculated. The weak-strong simulation is performed to demonstrate this idea.

INTRODUCTION

The EIC employs a local crabbing compensation scheme, as illustrated in Fig. 1, to attain the desired luminosity [1]. The scheme involves placing a set of crab cavities on either side of the interaction point (IP). The upstream cavity is utilized to tilt the beam in the $x-z$ plane, while the downstream cavity is employed to restore the beam's original orientation. The remaining segments of the collider's ring are unaffected by this maneuver.

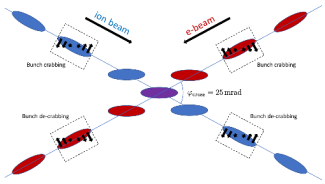

Figure 1: EIC local crabbing compensation scheme

The optimal local crabbing scheme necessitates the installation of two crab cavities at positions with betatron phase advances of ±90° from the IP to create the desired crab "bump" between them. The magnitude of the kick imparted by the crab cavity is inversely proportional to the square root of the beta function at the crab cavity location. A large value of beta function is essential to reduce the crab cavity voltage requirement. However, in the HSR of the EIC, the conflicting requirements of a large beta function and a specific phase advance at the crab cavities, with the constraints on the near-IR magnets [2], make it almost impractical to achieve crab bump closure with two crab cavities.

In the latest lattice design of the HSR, the phase advance between crabs is 5° short of 180°, which leaves the residual crabbing around the ring. The residual crabbing may have an negative impact on the dynamic aperture [3]. It is desirable to close the crab dispersion as locally as possible. The inclusion of a third crab cavity may facilitate the closure of the crabbing within the crabs. Unfortunately, there is no available space to install a third crab cavity in IR6, which is the collision zone of the EIC. Additionally, the installation of another crab cavity would introduce additional transverse and longitudinal impedance.

The residual crabbing may induce the linear synchro-betatron resonance. As reported in the literature [4], the existence of non-zero momentum dispersion at the accelerating cavity has the capability to excite synchro-betatron resonance too. This opens up a promising avenue to utilize the existing RF cavity to effect the closure of crabbing by introducing momentum dispersion at the RF cavity. In this paper, we shall investigate this notion. In the ensuing mathematical expressions, a calligraphic symbol shall be employed to denote a 6×6 matrix, whereas a standard font shall be used to signify the 4×4 block.

CRAB DISPERSION

The Hamiltonian of a thin crab cavity is

$$H = \left(\frac{x\lambda_x}{\Lambda_x} + \frac{y\lambda_y}{\Lambda_y}\right)\frac{\sin(k_c z)}{k_c}, \tag{1}$$

where x, y, z are the horizontal, vertical, and longitudinal coordinates when a test particle pass through the thin crab cavity, $\lambda_{x,y}/\Lambda_{x,y}$ denoting the horizontal and vertical kick strength with $\Lambda_x = \sqrt{\beta_x^*\beta_{x,c}}, \Lambda_y = \sqrt{\beta_y^*\beta_{y,c}}$, and k_c the wave number. Here we use the lattice related parameters $\Lambda_{x,y}$ to normalize the crab cavity strength for simplicity.

Following the definition in [5], the crab dispersion is defined as the transverse dependence on longitudinal coordinate z,

$$\boldsymbol{\zeta} = \left(\frac{\partial x}{\partial z}, \frac{\partial p_x}{\partial z}, \frac{\partial y}{\partial z}, \frac{\partial p_y}{\partial z}\right)^{\mathrm{T}}. \tag{2}$$

The crab dispersion generated by the thin crab cavity is,

$$\boldsymbol{\zeta} = \left(0, \lambda_x/\Lambda_x, 0, \lambda_y/\Lambda_y\right)^{\mathrm{T}}. \tag{3}$$

* Work supported by Brookhaven Science Associates, LLC under Contract No. DE-SC0012704 with the U.S. Department of Energy
† dxu@bnl.gov

ISBN: 978-3-95450-231-8 ISSN: 2673-5490 doi: 10.18429/JACoW-IPAC2023-MOPA040

By employing the crab dispersion, the transverse coordinates (x, p_x, y, p_y) can be decoupled from the longitudinal offset z. Let $\mathcal{R}$ be the one-turn transfer matrix expressed as a 6×6 matrix with the following form:

$$\mathcal{R} = \begin{bmatrix} r_{11} & r_{12} & r_{13} & r_{14} & r_{15} & 0 \\ r_{21} & r_{22} & r_{23} & r_{24} & r_{25} & 0 \\ r_{31} & r_{32} & r_{33} & r_{34} & r_{35} & 0 \\ r_{41} & r_{42} & r_{43} & r_{44} & r_{45} & 0 \\ 0 & 0 & 0 & 0 & 1 & 0 \\ r_{61} & r_{62} & r_{63} & r_{64} & r_{65} & 1 \end{bmatrix}. \tag{4}$$

It is possible to diagonalize $\mathcal{R}$ as follows:

$$\mathcal{R} = \mathcal{M}_\zeta \begin{bmatrix} r_{11} & r_{12} & r_{13} & r_{14} & 0 & 0 \\ r_{21} & r_{22} & r_{23} & r_{24} & 0 & 0 \\ r_{31} & r_{32} & r_{33} & r_{34} & 0 & 0 \\ r_{41} & r_{42} & r_{43} & r_{44} & 0 & 0 \\ 0 & 0 & 0 & 0 & 1 & 0 \\ 0 & 0 & 0 & 0 & \bar{r}_{65} & 1 \end{bmatrix} . \mathcal{M}_\zeta^{-1} \tag{5}$$

Here, $\mathcal{M}_\zeta$ is a symplectic matrix and takes the form of:

$$\mathcal{M}_\zeta = \begin{bmatrix} \mathbf{1}_{4\times4} & \boldsymbol{\zeta} & \mathbf{0}_{4\times1} \\ \mathbf{0}_{1\times4} & 1 & 0 \\ (J\boldsymbol{\zeta})^{\mathrm{T}} & 0 & 1 \end{bmatrix}, \tag{6}$$

where J is the 4×4 symplectic form matrix

$$J = \begin{bmatrix} 0 & 1 & 0 & 0 \\ -1 & 0 & 0 & 0 \\ 0 & 0 & 0 & 1 \\ 0 & 0 & -1 & 0 \end{bmatrix}. \tag{7}$$

Similarly, if $\mathcal{R}$ takes the form of

$$\mathcal{R} = \begin{bmatrix} r_{11} & r_{12} & r_{13} & r_{14} & 0 & r_{16} \\ r_{21} & r_{22} & r_{23} & r_{24} & 0 & r_{26} \\ r_{31} & r_{32} & r_{33} & r_{34} & 0 & r_{33} \\ r_{41} & r_{42} & r_{43} & r_{44} & 0 & r_{46} \\ r_{51} & r_{52} & r_{53} & r_{54} & 1 & r_{56} \\ 0 & 0 & 0 & 0 & 0 & 1 \end{bmatrix}. \tag{8}$$

$\mathcal{R}$ can be diagonalized with the concept of momentum dispersion $\boldsymbol{\eta}$

$$\mathcal{R} = \mathcal{M}_\eta \begin{bmatrix} r_{11} & r_{12} & r_{13} & r_{14} & 0 & 0 \\ r_{21} & r_{22} & r_{23} & r_{24} & 0 & 0 \\ r_{31} & r_{32} & r_{33} & r_{34} & 0 & 0 \\ r_{41} & r_{42} & r_{43} & r_{44} & 0 & 0 \\ 0 & 0 & 0 & 0 & 1 & \bar{r}_{56} \\ 0 & 0 & 0 & 0 & 0 & 1 \end{bmatrix} \mathcal{M}_\eta^{-1}, \tag{9}$$

where the symplectic matrix $\mathcal{M}_\eta$ is

$$\mathcal{M}_\eta = \begin{bmatrix} \mathbf{1}_{4\times4} & \mathbf{0}_{4\times1} & \boldsymbol{\eta} \\ -(J\boldsymbol{\eta})^{\mathrm{T}} & 1 & 0 \\ \mathbf{0}_{1\times4} & 0 & 1 \end{bmatrix}. \tag{10}$$

The crab dispersion $\boldsymbol{\zeta}$ or momentum dispersion $\boldsymbol{\eta}$ can be resolved from the Eq. (5) or Eq. (9),

$$\boldsymbol{\zeta} = (I - R)^{-1}(r_{15}, r_{25}, r_{35}, r_{45})^{\mathrm{T}} \tag{11}$$

$$\boldsymbol{\eta} = (I - R)^{-1}(r_{16}, r_{26}, r_{36}, r_{46})^{\mathrm{T}}, \tag{12}$$

where R is the 4×4 block in Eq. (4) or Eq. (13).

For a general form of $\mathcal{R}$,

$$\mathcal{R} = \begin{bmatrix} r_{11} & r_{12} & r_{13} & r_{14} & r_{15} & r_{16} \\ r_{21} & r_{22} & r_{23} & r_{24} & r_{25} & r_{26} \\ r_{31} & r_{32} & r_{33} & r_{34} & r_{35} & r_{33} \\ r_{41} & r_{42} & r_{43} & r_{44} & r_{45} & r_{46} \\ r_{51} & r_{52} & r_{53} & r_{54} & r_{55} & r_{56} \\ r_{61} & r_{62} & r_{63} & r_{64} & r_{65} & r_{66} \end{bmatrix}. \tag{13}$$

we can make a succession of the two canonical transformations $\mathcal{M}_\zeta$ and $\mathcal{M}_\eta$ to diagonalize $\mathcal{R}$ [6],

$$\mathcal{R} = \mathcal{M}_\zeta \mathcal{M}_\eta \begin{bmatrix} \bar{r}_{11} & \bar{r}_{12} & \bar{r}_{13} & \bar{r}_{14} & 0 & 0 \\ \bar{r}_{21} & \bar{r}_{22} & \bar{r}_{23} & \bar{r}_{24} & 0 & 0 \\ \bar{r}_{31} & \bar{r}_{32} & \bar{r}_{33} & \bar{r}_{34} & 0 & 0 \\ \bar{r}_{41} & \bar{r}_{42} & \bar{r}_{43} & \bar{r}_{44} & 0 & 0 \\ 0 & 0 & 0 & 0 & \bar{r}_{55} & \bar{r}_{56} \\ 0 & 0 & 0 & 0 & \bar{r}_{65} & \bar{r}_{66} \end{bmatrix} \mathcal{M}_\eta^{-1} \mathcal{M}_\zeta^{-1} \tag{14}$$

$\boldsymbol{\zeta}$ and $\boldsymbol{\eta}$ can be determined from the above equation numerically.

From Hirata [7], the linear map for the Lorentz boost in the crab crossing scheme is

$$\mathcal{L} \approx \begin{bmatrix} 1 & 0 & 0 & 0 & \theta_c & 0 \\ 0 & 1 & 0 & 0 & 0 & 0 \\ 0 & 0 & 1 & 0 & 0 & 0 \\ 0 & 0 & 0 & 1 & 0 & 0 \\ 0 & 0 & 0 & 0 & 1 & 0 \\ 0 & -\theta_c & 0 & 0 & 0 & 1 \end{bmatrix}, \tag{15}$$

where θ_c is the half crossing angle, and the approximation $\theta_c \approx 0$ is used. The linear Lorentz boost $\mathcal{L}$ is literally a crab transformation with $\boldsymbol{\zeta} = (\theta_c, 0, 0, 0)^{\mathrm{T}}$. To provide an effective head-on collision, the crab dispersion and the momentum dispersion are found to be

$$\mathcal{L}\mathcal{M}_\zeta \mathcal{M}_\eta = \mathbf{1}_{6\times6} \Longrightarrow \boldsymbol{\zeta}_b^* = (-\theta_c, 0, 0, 0)^{\mathrm{T}},\ \boldsymbol{\eta}_b^* = \mathbf{0}_{4\times1} \tag{16}$$

where the superscript symbol "*" denotes IP, and the subscript "b" indicates before collision. The crab dispersion bump is closed if and only if,

$$\boldsymbol{\zeta}_a^* = \mathbf{0}_{4\times1},\ \boldsymbol{\eta}_a^* = \mathbf{0}_{4\times1} \tag{17}$$

the subscript "a" indicates after collision and out of the crab cavities.

BEAM-BEAM SIMULATION

Weak-strong simulation is a widely used approach in beam-beam study [8, 9]. We use a self-written weak-strong

ISBN: 978-3-95450-231-8 ISSN: 2673-5490 doi: 10.18429/JACoW-IPAC2023-MOPA040

code to check the idea. A second order harmonic crab cavity is used to flatten the ion bunch [10]. The ion bunch is cut into multiple slices. Each slice is represented by a 2D Gaussian distribution in $x-y$ plane. The weak electron beam are simulated by a number of macro particles. The beam-beam interaction is modeled by the Bassetti-Erskine formula [11].

Figure 2 shows the accelerator model used in the weak-strong simulation. Except the crab cavities and the RF cavity, other elements are represented by a linear transfer matrix.

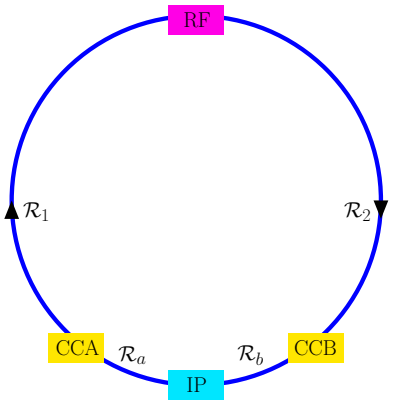

Figure 2: A simple accelerator model in the weak-strong simulation. "CCB" stands for the crab cavity before IP, and $\mathcal{R}_b$ is the transfer matrix from CCB to IP. "CCA" stands for the crab cavity after IP, and $\mathcal{R}_a$ is the transfer matrix from IP to CCA. "RF" stands for the RF cavity, and $\mathcal{R}_1$ is the transfer matrix from CCA to RF, while $\mathcal{R}_2$ is the transfer matrix from RF to CCB.

When the crab cavities are turned off, the one-turn transfer matrix at IP is,

$$\mathcal{R}_t = \mathcal{R}_b\mathcal{R}_2\mathcal{R}_{\rm rf}\mathcal{R}_1\mathcal{R}_a. \tag{18}$$

Without the distortion of the crab cavities, the x-y-z motion is completely decoupled.

When the crab cavities are turned on, the one-turn transfer matrix before/after collision is

$$\mathcal{R}_{t,b} = \mathcal{R}_b C_b \mathcal{R}^{-1}\mathcal{R}_t\mathcal{R}_a^{-1}C_a\mathcal{R}_a \tag{19}$$

$$\mathcal{R}_{t,a} = \mathcal{R}_a^{-1}C_a\mathcal{R}_a\mathcal{R}_b C_b\mathcal{R}^{-1}\mathcal{R}_t, \tag{20}$$

where $\mathcal{R}_{\rm rf}, C_b, C_a$ are the linear matrix for the RF, CCB and CCA in Fig. 2, respectively.

In order to simplify our computational analysis, we make the assumption that there is negligible momentum dispersion at the crab cavities, and that the $(\mathcal{R}_b\mathcal{R}_2)_{56}$ component from RF to IP is zero. By utilizing Eq. (14) to diagonalize the matrices $\mathcal{R}_{t,b}$ and $\mathcal{R}_{t,a}$, and satisfying the conditions specified in Eqs. (16) and (17), a potential solution to close the crabbing within the cavities is

$$\Psi_{\rm rf} = 90^\circ,\ d = -\frac{1}{q}\sqrt{\frac{\beta_{\rm rf}}{\beta^*}}\left(\cot\Psi_a + \cot\Psi_b\right),\ d' = 0. \tag{21}$$

where $\Psi_{\rm rf}$ is the phase advance from the RF to IP, Ψ_b the phase advance from CCB to IP, Ψ_a the phase advance from IP to CCA, and q denotes the RF cavity strength $q = (C_{\rm rf})_{65}$. d and d' are the momentum dispersion at the RF cavity.

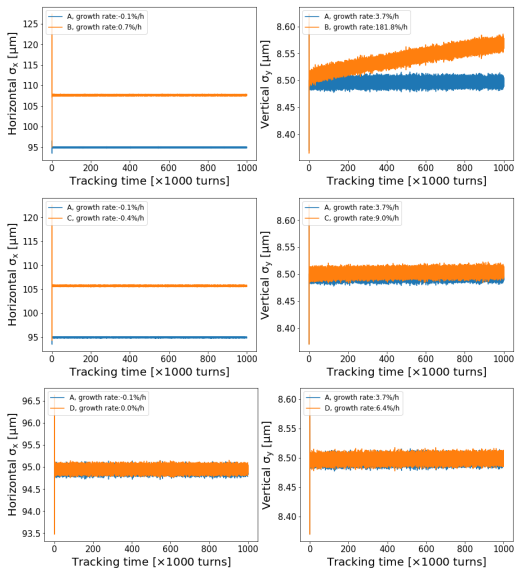

Figure 3: Beam size evolution by weak-strong simulation. Case A is the reference: $\Psi_b = \Psi_a = 90^\circ$. In case B, C, and D, $\Psi_b = 87^\circ$, $\Psi_a = 88^\circ$. The momentum dispersion at RF in case D is calculated from Eq. (21).

The outcomes of the simulation are presented in Fig. 3, depicting four distinct scenarios. Case A corresponds to a situation where there is no leakage of crab dispersion. Case A serves as the benchmark reference against which other cases are compared. In Cases B, C, and D, the phase advances are set to $\Psi_b = 87^\circ, \Psi_a = 88^\circ$.

In Case B, the crab cavity voltage is chosen as

$$\lambda_b^B = \frac{\theta_c}{\sin\Psi_b}, \qquad \lambda_a^B = \frac{\theta_c}{\sin\Psi_a}. \tag{22}$$

In this instance, neither of the conditions outlined in Eqs. (16) and (17) are satisfied. Consequently, a considerable growth is observed in the vertical plane.

In case C, the crab voltage is adjusted so that the condition Eq. (16) is satisfied while the condition Eq. (17) is not.

$$\begin{aligned}\lambda_b^C &= \frac{2\theta_c\sin\left(\Psi_a - \pi\nu_x\right)\sin\left(\pi\nu_x\right)}{\sin\left(\Psi_b + \Psi_a - 2\pi\nu_x\right)},\\ \lambda_a^C &= \frac{2\theta_c\sin\left(\Psi_b - \pi\nu_x\right)\sin\left(\pi\nu_x\right)}{\sin\left(\Psi_b + \Psi_a - 2\pi\nu_x\right)},\end{aligned} \tag{23}$$

where ν_x denotes the horizontal tune. Now the vertical growth is eliminated. However, the horizontal size increases about 10 μm after equilibrium.

In case D, the crab voltage is same as in case B, $\lambda_b^D = \lambda_b^B, \lambda_a^D = \lambda_a^D$. We introduce additional momentum dispersion at RF cavity in case D. The value is shown in Eq. (21). We can see that the curves A and D overlap with each other. The crab dispersion is perfectly closed by the RF cavity.

ISBN: 978-3-95450-231-8 ISSN: 2673-5490 doi: 10.18429/JACoW-IPAC2023-MOPA040

REFERENCES

[1] F. Willeke and J. Beebe-Wang, "Electron-Ion Collider Conceptual Design Report 2021", BNL, NY, USA, BNL-221006-2021-FORE, 2021. doi:10.2172/1765663

[2] J. S. Berg *et al.*, "Lattice Design for the Interaction Region of the Electron-Ion Collider ", presented at IPAC'23, Venice, Italy, 2023, paper WEPL030, this conference.

[3] Y. Luo *et al.*, "Simulation Test of Various Crab Dispersion Closure Bumps for the Hadron Storage Ring of the Electron-Ion Collider", presented at IPAC'23, Venice, Italy, 2023, paper MOPA045, this conference.

[4] A. Piwinski, "Synchro-betatron resonances", Lecture Notes in Physics: Nonlinear Dynamics Aspects of Particle Accelerators. Berlin, Heidelberg: Springer Berlin Heidelberg, 2007, pp. 104–120.

[5] Y.-P. Sun *et al.*, "Crab dispersion and its impact on the CERN Large Hadron Collider collimation", *Phys. Rev. ST Accel. Beams*, vol. 13, p. 031001, 2010. doi:10.1103/PhysRevSTAB.13.031001

[6] D. Xu *et al.*, "Combined effects of crab dispersion and momentum dispersion in colliders with local crab crossing scheme", *Phys. Rev. Accel. Beams*, vol. 25, p. 071002, 2022. doi:10.1103/PhysRevAccelBeams.25.071002

[7] K. Hirata, "Analysis of beam-beam interactions with a large crossing angle", *Phys. Rev. Lett.*, vol. 74, p. 2228, 1995. doi:10.1103/PhysRevLett.74.2228

[8] Y. Papaphilippou *et al.*, "Weak-strong beam-beam simulations for the Large Hadron Collider", *Phys. Rev. ST Accel. Beams*, vol. 2, p. 104001, 1999. doi:10.1103/PhysRevSTAB.2.104001

[9] Y. Luo *et al.*, "Six-dimensional weak-strong simulation of head-on beam-beam compensation in the Relativistic Heavy Ion Collider", *Phys. Rev. ST Accel. Beams*, vol. 15, p. 051004, 2012. doi:10.1103/PhysRevSTAB.15.051004

[10] D. Xu *et al.*, "Study of Harmonic Crab Cavity in EIC Beam-Beam Simulations", BNL, NY, USA, BNL-222291-2021-COPA, 2021.

[11] M. Bassetti and G. A. Erskine, "Closed expression for the electrical field of a two-dimensional Gaussian charge", Tech. Report No. ISR-TH-80-06, 1980.